

Kink interactions in $SU(N) \times Z_2$

Levon Pogossian

*Theoretical Physics, The Blackett Laboratory, Imperial College,
Prince Consort Road, London SW7 2BZ, United Kingdom.*

There are $N - 1$ classes of kink solutions in $SU(N) \times Z_2$. We show how interactions between various kinks depend on the classes of individual kinks as well as on their orientations with respect to each other in the internal space. In particular, we find that the attractive or repulsive nature of the interaction depends on the trace of the product of charges of the two kinks. We calculate the interaction potential for all combinations of kinks and antikinks in $SU(5) \times Z_2$ and study their collisions. The outcome of kink-antikink collisions, as expected from previous studies, is sensitive to their initial relative velocity. We find that heavier kinks tend to break up into lighter ones, while interactions between the lightest kinks and antikinks in this model can be repulsive as well as attractive.

I. INTRODUCTION

Topological defects are observed in condensed matter systems and may have been formed during phase transitions¹ at early stages in the history of the universe [1]. If observed, they would provide invaluable information about the universe when it was a tiny fraction of a second old. If not observed, topological defects still play an important role by placing constraints on particle physics models and cosmology. The formation and scaling of a network of defects strongly depends on how they interact among themselves. This, in turn, will affect the type and the strength of restrictions that observations (or the lack thereof) can impose on the underlying model. Another context, in which interactions between defects are important, is the possible connection between elementary particles and solitonic solutions of classical field equations [2].

In addition to the more general reasons given above, understanding how the $SU(N) \times Z_2$ domain walls interact could be important in the light of the correspondence, found by Vachaspati [3], between the spectrum of $SU(5)$ monopoles and the spectrum of one family of fermions in the Standard Model. Interactions between $SU(N) \times Z_2$ kinks may also be relevant to the solution of the monopole over-abundance problem based on sweeping monopoles with domain walls as proposed in [4].

Previous work on interactions between kinks has mainly concentrated on the sine-Gordon and the ϕ^4 models in (1+1) dimensions [5, 6, 7, 8, 9, 10, 11, 12]. Even a relatively simple system of a ϕ^4 kink interacting with an antikink can have rather non-trivial dynamics, which is one of the reasons why so many researchers have worked on this problem in the past. The force between kinks and antikinks of the ϕ^4 model is always attractive. The outcome of their collision can be one of the three types: they can annihilate, they can scatter off each other or they can form an intermediate bound state before ultimately sep-

arating or annihilating. The general tendency is that at low collision velocities kinks tend to annihilate and at higher velocities they scatter. However, the dependence of the outcome on the incident velocity is rather nonlinear, as was found in [5, 6, 7, 8, 9, 10] and investigated in detail in [12]. Namely, it was found that, over a relatively small range of initial velocities, intervals of initial velocity for which kink and antikink capture each other alternate with regions for which the interaction concludes with escape to infinite separations. In [12], this alternation phenomenon was attributed to a nonlinear resonance between the orbital frequency of the bound kink-antikink pair and the frequency of characteristic small oscillations of the field localized at the moving kink and antikink centers.

In this work, when discussing interactions between kinks, we will aim to concentrate on issues that are unique to $SU(N) \times Z_2$ and will refer to earlier work when a problem can be reduced to that of kinks in the ϕ^4 model. In particular, we will show that in $SU(N) \times Z_2$ kinks can repel as well as attract.

This paper is organized as follows. In Sec. II we give a brief overview of kink solutions in $SU(N) \times Z_2$. In Sec. III we develop a framework in which $SU(N) \times Z_2$ kink interactions can be discussed and show a simple way of determining whether a given pair of kinks will attract or repel. In Sections IV and V we study the kink-antikink interactions in $SU(5) \times Z_2$. Results are summarized in Sec. VI

II. KINKS IN $SU(N) \times Z_2$

Consider a (1+1)-dimensional model of a scalar field Φ transforming in the adjoint representation of $SU(N)$, with N taken to be odd and with the additional Z_2 symmetry that takes Φ to $-\Phi$. The Lagrangian is

$$L = \text{Tr}(\partial_\mu \Phi)^2 - V(\Phi), \quad (1)$$

¹ Here, the term “phase transition” includes continuous transitions called crossovers.

where $V(\Phi)$ is such that Φ has an expectation value Φ_V that can be chosen to be

$$\Phi_V = \eta \sqrt{\frac{2}{N(N^2-1)}} \begin{pmatrix} n\mathbf{1}_{n+1} & \mathbf{0} \\ \mathbf{0} & -(n+1)\mathbf{1}_n \end{pmatrix}, \quad (2)$$

where $\mathbf{1}_p$ is the $p \times p$ identity matrix, $N \equiv 2n+1$ and η is an energy scale determined by the minima of the potential V . Such an expectation value spontaneously breaks the symmetry down to:

$$H = [SU(n+1) \times SU(n) \times U(1)]/[Z_{n+1} \times Z_n]. \quad (3)$$

Various types of kink solutions in this model are defined by choices of the boundary conditions at $x = -\infty$ and $x = +\infty$, where x is the space coordinate. It was proved in [13] that for a kink solution to exist one must necessarily have $[\Phi(-\infty), \Phi(+\infty)] = 0$. This allows one to list all the possible boundary conditions (up to gauge rotations) that can lead to kink solutions. We can fix $\Phi_L \equiv \Phi(-\infty) = \Phi_V$ given in Eq. (2). Then we can have

$$\Phi_R \equiv \Phi(+\infty) = \epsilon_T \eta \sqrt{\frac{2}{N(N^2-1)}} \times$$

$$\text{diag}(n\mathbf{1}_{n+1-q}, -(n+1)\mathbf{1}_q, n\mathbf{1}_q, -(n+1)\mathbf{1}_{n-q}), \quad (4)$$

where we have introduced a parameter $\epsilon_T = \pm 1$ and another $q = 0, \dots, n$. The label ϵ_T is $+1$ when the boundary conditions are topologically trivial and is -1 when they are topologically non-trivial. q tells us how many diagonal entries of Φ_L have been permuted in Φ_R . The case $q = 0$ is when $\Phi_R = \epsilon_T \Phi_L$. As was suggested in [13], the lowest energy stable topological ($\epsilon_T = -1$) kink solution corresponds to $q = n$. Topological $q = n$ kinks were studied in detail in [15, 16].

The most general ansatz for the kink solution was found in [13] and can be written as:

$$\Phi_k = F_+(x)\mathbf{M}_+ + F_-(x)\mathbf{M}_- + g(x)\mathbf{M}, \quad (5)$$

where

$$\mathbf{M}_+ = \frac{\Phi_R + \Phi_L}{2}, \quad \mathbf{M}_- = \frac{\Phi_R - \Phi_L}{2}. \quad (6)$$

and, for $q \neq 0$ and $q \neq n$,

$$\mathbf{M} = \mu \text{diag}(q(n-q)\mathbf{1}_{n+1-q}, -(n-q)(n+1-q)\mathbf{1}_q, \\ -(n-q)(n+1-q)\mathbf{1}_q, q(n+1-q)\mathbf{1}_{n-q}) \quad (7)$$

with

$$\mu = \eta [2q(n-q)(n+1-q)\{2n(n+1-q) - q\}]^{-1/2}. \quad (8)$$

For $q = 0$ or for $q = n$, the matrix \mathbf{M} is zero. The boundary conditions for F_{\pm} and $g(x)$ are:

$$F_{-}(\pm\infty) = \pm 1, \quad F_{+}(\pm\infty) = 1, \quad g(\pm\infty) = 0. \quad (9)$$

One can define the charge of the kinks as [2]

$$Q \equiv \frac{1}{\eta} (\Phi_k(+\infty) - \Phi_k(-\infty)), \quad (10)$$

which corresponds to a current

$$j^{\mu} \equiv \frac{1}{\eta} \varepsilon^{\mu\nu} \partial_{\nu} \Phi, \quad (11)$$

where $\mu, \nu = 0, 1$, and $\varepsilon^{\mu\nu}$ is the antisymmetric tensor. The definition (10) of Q can be used for non-topological kinks as well as topological ones.

III. KINK INTERACTIONS IN $SU(N) \times Z_2$

Consider two kinks, $K^{(1)}$ and $K^{(2)}$, separated by a distance which is larger than their core sizes. The classes to which the two kinks belong, as well as the global topology of the two-kink configuration, are determined by the choices of the three vacua:

- Φ_- at $x = -\infty$,
- Φ_0 in between the two kinks,
- Φ_+ at $x = +\infty$.

Let indices $(\epsilon_T^{(1)}, q^{(1)})$ describe the kink between Φ_- and Φ_0 , where $q^{(1)}$ denotes the kink class as defined in Sec. II, and $\epsilon_T^{(1)}$ is -1 for topological and $+1$ for non-topological kinks. Similarly, let $(\epsilon_T^{(2)}, q^{(2)})$ denote the kink bounded by Φ_0 and Φ_+ . Boundaries Φ_- and Φ_+ of the two-kink system can also be described using indices $(\epsilon_T^{(3)}, q^{(3)})$ defined in a similar way. Topology requires that $\epsilon_T^{(3)} = \epsilon_T^{(1)} \epsilon_T^{(2)}$. Thus, the two-kink system can be described by $(q^{(1)}, q^{(2)}, q^{(3)}, \epsilon_T^{(1)}, \epsilon_T^{(2)})$. This notation is invariant under global gauge rotations, since it contains only information about how many diagonal entries were permuted in each of the vacua Φ_- , Φ_0 and Φ_+ with respect to each other.

For given values of $q^{(1)}$ and $q^{(2)}$, not all values of $q^{(3)}$ will generally be allowed. To determine the selection procedure, let us start with Φ_0 , in which $q^{(1)}$ diagonal entries of Φ_- were permuted. We want to know how many diagonal entries of Φ_- can be permuted in Φ_+ (i.e. the value of $q^{(3)}$) given that $q^{(2)}$ diagonal entries of Φ_0 were permuted in Φ_+ . There are $n+1$ entries with absolute values equal to n in Φ_- (see Eq. (2)), which we can denote by \mathcal{A} 's, and n entries with absolute values equal to $(n+1)$, which we will denote by \mathcal{B} 's. We will refer to those \mathcal{A} 's and \mathcal{B} 's of Φ_0 , that were permuted to form Φ_0 out of Φ_- , as "changed", and the ones that were left untouched as "unchanged". Then, when permuting \mathcal{A} 's and \mathcal{B} 's of Φ_0 to form Φ_+ ($q^{(2)}$ permutations), one has the following options:

1. Permute a changed \mathcal{A} with a changed \mathcal{B} . This operation will decrease the value of $q^{(3)}$ by 1, since it will restore the original order of the given pair of \mathcal{A} and \mathcal{B} in Φ_- . Let $q_1^{(2)}$ denote the number of possible ways it can be done. Since there are only $q^{(1)}$ changed \mathcal{A} 's, $q_1^{(2)} \leq \min(q^{(1)}, q^{(2)})$. Also, if there is a deficit of unchanged \mathcal{A} 's, one is forced to permute at least $(q^{(2)} - n + q^{(1)} - 1)$ changed \mathcal{A} 's, which means that $q_1^{(2)} \geq \max(0, q^{(2)} - n + q^{(1)} - 1)$.
2. Permute a changed \mathcal{A} with an unchanged \mathcal{B} . This operation does not affect the value of $q^{(3)}$. The number of possible ways in which this can be done, denoted by $q_2^{(2)}$, is limited by the number of available changed \mathcal{A} 's and unchanged \mathcal{B} 's: $q_2^{(2)} \leq \min(q^{(1)} - q_1^{(2)}, n - q^{(1)})$.
3. Permute an unchanged \mathcal{A} with a changed \mathcal{B} . This operation also does not change the value of $q^{(3)}$. It can be done in $q_3^{(2)}$ ways, limited by the number of available unchanged \mathcal{A} 's and changed \mathcal{B} 's: $q_3^{(2)} \leq \min(n - q^{(1)} + 1, q^{(1)} - q_1^{(2)})$.
4. Permute an unchanged \mathcal{A} with an unchanged \mathcal{B} . This operation will increase the value of $q^{(3)}$ by 1, and can be performed in $q_4^{(2)}$ ways, limited by the number of available unchanged \mathcal{A} 's and unchanged \mathcal{B} 's: $q_4^{(2)} \leq \min(n - q^{(1)} - q_3^{(2)} + 1, n - q^{(1)} - q_2^{(2)})$.

In summary, independent of $\epsilon_T^{(1)}$ and $\epsilon_T^{(2)}$, given $q^{(1)}$ and $q^{(2)}$, the set of possible values of $q^{(3)}$ can be found using

$$q^{(3)} = q^{(1)} - q_1^{(2)} + q_4^{(2)}, \quad (12)$$

where we have defined integers $q_i^{(2)}$ ($i = 1, 2, 3, 4$) that can take on all non-negative values allowed by the following selection rules:

$$\begin{aligned} q_1^{(2)} + q_2^{(2)} + q_3^{(2)} + q_4^{(2)} &= q^{(2)}, \\ \max(0, q^{(2)} - n + q^{(1)} - 1) &\leq q_1^{(2)} \leq \min(q^{(1)}, q^{(2)}), \\ 0 &\leq q_2^{(2)} \leq \min(q^{(1)} - q_1^{(2)}, n - q^{(1)}), \\ 0 &\leq q_3^{(2)} \leq \min(n - q^{(1)} + 1, q^{(1)} - q_1^{(2)}), \\ 0 &\leq q_4^{(2)} \leq \min(n - q^{(1)} - q_3^{(2)} + 1, n - q^{(1)} - q_2^{(2)}). \end{aligned} \quad (13)$$

Next we would like to determine whether a given pair of kinks will attract or repel. We can use a procedure which is analogous to one used by Manton [14] in the case of the ϕ^4 . At large separations, the two-kink ansatz can be written as:

$$\Phi(x) = \Phi_k^{(1)}(x+a) + \Phi_k^{(2)}(x-a) - \Phi_0, \quad (14)$$

where $\Phi_k^{(1)}(x)$ is the first kink solution with $\Phi_k^{(1)}(-\infty) = \Phi_-$, $\Phi_k^{(2)}(x)$ is the second kink solution with $\Phi_k^{(2)}(+\infty) = \Phi_+$, $\Phi_0 \equiv \Phi_k^{(1)}(+\infty) = \Phi_k^{(2)}(-\infty)$ is the vacuum in the

region separating the kinks and $a > 0$ is the distance from the origin to the centers of the kinks. Using Eqns. (5) and (10), we can write:

$$\begin{aligned} \Phi(x) &= F_+^{(1)} M_+^{(1)} + \frac{\eta}{2} F_-^{(1)} Q^{(1)} + g^{(1)} M^{(1)} \\ &+ F_+^{(2)} M_+^{(2)} + \frac{\eta}{2} F_-^{(2)} Q^{(2)} + g^{(2)} M^{(2)} - \Phi_0. \end{aligned} \quad (15)$$

In [13] it was shown that functions $F_+^{(1,2)}$ and $g^{(1,2)}$ can be treated as approximately constant for a relatively wide range of parameters of a general quartic potential. A simplified (and, therefore, only approximate) version of the two-kink ansatz is given by:

$$\begin{aligned} \Phi(x) &\approx M_+^{(1)} + \frac{\eta}{2} F_-^{(1)} Q^{(1)} \\ &+ M_+^{(2)} + \frac{\eta}{2} F_-^{(2)} Q^{(2)} - \Phi_0, \end{aligned} \quad (16)$$

where

$$M_+^{(1)} \equiv \frac{\Phi_- + \Phi_0}{2}, \quad M_+^{(2)} \equiv \frac{\Phi_0 + \Phi_+}{2}, \quad (17)$$

and

$$F_-^{(1)} \approx \tanh[\sigma(x+a)], \quad F_-^{(2)} \approx \tanh[\sigma(x-a)], \quad (18)$$

where $a \gg \sigma^{-1}$ and σ^{-1} is the "width" of the wall.

The field energy-momentum tensor can be derived using the action principle and is given by

$$T^{\mu\nu} = 2\text{Tr}[\partial^\mu \Phi \partial^\nu \Phi] - \eta^{\mu\nu} \text{Tr}[\partial^\sigma \Phi \partial_\sigma \Phi] - \eta^{\mu\nu} V(\Phi). \quad (19)$$

Therefore, the momentum density in (1+1) dimensions is

$$\mathcal{P} \equiv T_0^1 = -2\text{Tr}[\dot{\Phi} \Phi'], \quad (20)$$

where $\dot{\Phi} \equiv \partial_t \Phi$ and $\Phi' \equiv \partial_x \Phi$. One can define the momentum of a field configuration on the interval $x_1 < x < x_2$ as

$$P = - \int_{x_1}^{x_2} 2\text{Tr}[\dot{\Phi} \Phi'] dx. \quad (21)$$

To calculate the force between the kinks, let us consider the initial rate of change of momentum of a (initially) static field configuration given by the two-kink ansatz:

$$\frac{dP}{dt} = - \int_{x_1}^{x_2} 2(\text{Tr}[\ddot{\Phi} \Phi'] + \text{Tr}[\dot{\Phi} \Phi'']) dx. \quad (22)$$

One can use field equations of motion and integrate to obtain

$$\frac{dP}{dt} = \left[-\text{Tr}[\dot{\Phi}^2] - \text{Tr}[(\Phi')^2] + V(\Phi) \right]_{x_1}^{x_2}. \quad (23)$$

Let us choose $x_1 \ll -a$ and $-a \ll x_2 \ll a$ (e. g. $x_2 = 0$). That is, we want to estimate the force on the first kink

(the one at $x = -a$), due to the second kink. Let us define

$$f \equiv \tanh[\sigma(x+a)] \quad \text{and} \quad \chi \equiv \tanh[\sigma(x-a)] + 1. \quad (24)$$

The two-kink ansatz given by (15) can then be re-written as

$$\Phi(x) \approx \frac{\Phi_- + \Phi_+}{2} + \frac{\eta}{2} Q^{(1)} f + \frac{\eta}{2} Q^{(2)} (-1 + \chi). \quad (25)$$

Initially, $\dot{\Phi} = 0$. Also, within the range $x_1 < x < x_2$, $\chi(x) \ll 1$ and we can perform an expansion in χ . To the leading order in χ we find:

$$\begin{aligned} \frac{dP}{dt} \approx & \left[-\frac{\eta^2}{4} \text{Tr}[(Q^{(1)})^2] (f')^2 - \frac{\eta^2}{2} \text{Tr}[Q^{(1)} Q^{(2)}] f' \chi' \right. \\ & \left. + [V]_{\chi=0} + \sum_a \left[\frac{\partial V}{\partial \Phi^a} \right]_{\chi=0} \chi^a \right]_{x_1}^{x_2}, \end{aligned} \quad (26)$$

where functions χ^a are defined by

$$\chi^a \equiv \frac{\eta}{2} [Q^{(2)}]^a \chi \quad (27)$$

and coefficients $[Q^{(2)}]^a$ are defined by

$$Q^{(2)} = \sum_a [Q^{(2)}]^a T^a, \quad (28)$$

where T^a are the $SU(N)$ generators normalized so that $\text{Tr}[T^a T^b] = \delta_{ab}/2$. Using the equations of motion gives

$$\begin{aligned} \frac{dP}{dt} \approx & \left[-\frac{\eta^2}{2} \text{Tr}[Q^{(1)} Q^{(2)}] f' \chi' + \sum_a [\Phi^{a''}]_{\chi=0} \chi^a \right]_{x_1}^{x_2} \\ = & \frac{\eta^2}{2} \text{Tr}[Q^{(1)} Q^{(2)}] \left[-f' \chi' + f'' \chi \right]_{x_1}^{x_2}. \end{aligned} \quad (29)$$

It can be shown that $\left[-f' \chi' + f'' \chi \right]_{x_1}^{x_2} < 0$ for all x_1 and x_2 satisfying the constraints. Thus, the sign of dP/dt , and the attractive or repulsive nature of the force, is determined by the sign of $\text{Tr}[Q^{(1)} Q^{(2)}]$.

Next we would like to express $\text{Tr}[Q^{(1)} Q^{(2)}]$ in terms of parameters $(q^{(1)}, q^{(2)}, q^{(3)}, \epsilon_T^{(1)}, \epsilon_T^{(2)})$ which define the two-kink configuration. We write

$$\begin{aligned} \text{Tr}[Q^{(1)} Q^{(2)}] = & \frac{1}{\eta^2} (\text{Tr}[\Phi_- \Phi_0] + \text{Tr}[\Phi_0 \Phi_+]) \\ & - \text{Tr}[\Phi_- \Phi_+] - \text{Tr}[\Phi_0 \Phi_0]. \end{aligned} \quad (30)$$

Applying definitions (2) and (4) to boundary conditions specified by (Φ_L, Φ_R) we find:

$$\begin{aligned} \frac{1}{\eta^2} \text{Tr}[\Phi_L \Phi_R] = & \frac{2\epsilon_T}{N(N^2 - 1)} [(n+1-q)n^2 \\ & - 2q^{(1)}(n+1)n + (n-q)(n+1)^2] \\ = & \frac{\epsilon_T}{2} \left[1 - q \frac{(2n+1)}{n(n+1)} \right]. \end{aligned} \quad (31)$$

Using the above expression and the fact that $\text{Tr}[\Phi_0 \Phi_0] = \eta^2/2$ we find:

$$\begin{aligned} \text{Tr}[Q^{(1)} Q^{(2)}] = & \frac{1}{2} (\epsilon_T^{(1)} + \epsilon_T^{(2)} - \epsilon_T^{(1)} \epsilon_T^{(2)} - 1) \\ & - (\epsilon_T^{(1)} q^{(1)} + \epsilon_T^{(2)} q^{(2)} - \epsilon_T^{(1)} \epsilon_T^{(2)} q^{(3)}) \frac{(2n+1)}{2n(n+1)}. \end{aligned} \quad (32)$$

One can see, for example, that in the case of a topological kink interacting with a topological antikink ($\epsilon_T^{(1)} = -1$ and $\epsilon_T^{(2)} = -1$) both, attraction and repulsion, are possible depending on the choices of $q^{(1)}$, $q^{(2)}$ and $q^{(3)}$. This is a novel feature, when compared to the classical ϕ^4 case [2], where the force between a kink and an antikink is always attractive. An analogous situation is found in the case of interactions between global $O(3)$ monopoles [17]. There, attraction or repulsion between a monopole and an antimonopole is determined not by their topological charges but by the relative phase of their field configurations.

Our derivation of the fact that the sign of $\text{Tr}[Q^{(1)} Q^{(2)}]$ determines whether kinks will attract or repel was independent of a particular form of $V(\Phi)$. We did, however, rely on certain approximations in the derivation that may not be valid for some extreme choices of $V(\Phi)$. Our numerical investigation of kink interactions in $SU(5) \times Z_2$ with a general quartic potential has always yielded an agreement between the sign of $\text{Tr}[Q^{(1)} Q^{(2)}]$ and the overall sign of the interaction potential.

In the next section we consider the $N = 5$ case and study interactions between kinks and antikinks in more detail.

IV. KINK INTERACTIONS IN $SU(5) \times Z_2$

Let us consider the (1+1)-dimensional model of a scalar field Φ transforming in the adjoint representation of $SU(5) \times Z_2$. We will take the potential to be

$$V(\Phi) = -m^2 \text{Tr}[\Phi^2] + h(\text{Tr}[\Phi^2])^2 + \lambda \text{Tr}[\Phi^4] + V_0, \quad (33)$$

with parameters such that the vacuum expectation value (VEV) of Φ breaks the symmetry spontaneously to $[SU(3) \times SU(2) \times U(1)]/[Z_3 \times Z_2]$. This happens in the parameter range

$$\frac{h}{\lambda} > -\frac{7}{30}, \quad \lambda > 0. \quad (34)$$

The VEV can be chosen to be $\Phi_V = \eta \text{diag}(2, 2, 2, -3, -3)/(2\sqrt{15})$, where

$$\eta \equiv \frac{m}{\sqrt{\lambda'}} \quad (35)$$

and

$$\lambda' \equiv h + \frac{7}{30} \lambda. \quad (36)$$

$\text{Tr}[Q^{(1)}Q^{(2)}]$ for	$q^{(3)} = 0$	$q^{(3)} = 1$	$q^{(3)} = 2$
$q^{(1)} = 0, q^{(2)} = 0$	-2 (A)	×	×
$q^{(1)} = 0, q^{(2)} = 1$	×	$-\frac{7}{6}$ (A)	×
$q^{(1)} = 0, q^{(2)} = 2$	×	×	$-\frac{1}{3}$ (A)
$q^{(1)} = 1, q^{(2)} = 1$	$-\frac{7}{6}$ (A)	$-\frac{3}{4}$ (A)	$-\frac{1}{3}$ (A)
$q^{(1)} = 1, q^{(2)} = 2$	×	$-\frac{1}{3}$ (A)	$+\frac{1}{12}$ (R)
$q^{(1)} = 2, q^{(2)} = 2$	$-\frac{1}{3}$ (A)	$+\frac{1}{12}$ (R)	×

Table I: $\text{Tr}[Q^{(1)}Q^{(2)}]$ evaluated for different choices of the topological kink - topological antikink configuration in $SU(5)$. (A) denotes attractions, (R) - repulsion and \times - means that the arrangement is impossible.

The constant $V_0 = m^2\eta^2/4$ in Eq. (33) ensures that $V(\Phi_V) = 0$.

We will study interactions between topological kinks and antikinks ($\epsilon_T^{(1)} = -1$, $\epsilon_T^{(2)} = -1$) with all possible choices for indices $q^{(1)}$, $q^{(2)}$ and $q^{(3)}$, as defined in Section II. We will not consider interactions between non-topological kinks nor interactions of non-topological kinks with topological ones. Our initial configuration will be that of two well-separated solitons moving towards each other. From here on, we will label such configurations with three indices, $(q^{(1)}, q^{(2)}, q^{(3)})$, and it will be assumed that $\epsilon_T^{(1)} = \epsilon_T^{(2)} = -1$.

In this model, only the $q = 2$ topological kink solution is stable. It also has the smallest energy of all kinks. However, we will not restrict the analysis to $q = 2$ kinks, as interactions between all types of kinks antikinks could be potentially interesting.

We start by evaluating $\text{Tr}[Q^{(1)}Q^{(2)}]$ for all possible choices of the configuration of a kink and an antikink using Eq. (32). As we have shown in Section III, this should tell us whether the two kinks will attract or repel. The results are given in Table I and show that there are two possible combinations in which there is a repulsive force between the solitons.

We would like to evaluate the interaction energy between different classes of kinks and antikinks in $SU(5) \times Z_2$. The cases when analytical kink solutions are known are the $q = 0$ kink and, for the special value $h/\lambda = -3/20$, the $q = 2$ kink [15, 16]. The $q = 0$ kink solution is the same as in the ϕ^4 model, since in this case the only non-zero component of Φ is the one along Φ_V , that is $\Phi = \phi(x)\Phi_V/\eta$, and the potential takes the same form as in the ϕ^4 theory:

$$V = \frac{\lambda'}{4}(\phi^2 - \eta^2)^2. \quad (37)$$

Therefore, the interaction potential between $q = 0$ kinks and antikinks will be identical to the one found in the ϕ^4 model [10].

Let us next consider $q = 2$ kinks and antikinks. Consider a kink at $x = -a$ and an antikink at $x = a$, with

$a > 0$, each moving with a velocity v directed towards the origin. For values of a larger than the core sizes of two kinks the following ansatz is valid:

$$\Phi_{K\bar{K}}(x) = \Phi_K(x+a) + \Phi_{\bar{K}}(x-a) - \Phi_0, \quad (38)$$

where $\Phi_0 = \Phi_K(+\infty) = \Phi_{\bar{K}}(-\infty)$ is the field in between the two kinks. For $h = -3\lambda/20$ and $q = 2$ the kink solution is known [15, 16]:

$$\Phi_{q=2}(x) = \frac{[1 - \tanh(\sigma x)]}{2}\Phi_- + \frac{[1 + \tanh(\sigma x)]}{2}\Phi_+, \quad (39)$$

where $\sigma = m/\sqrt{2}$. The ansatz for the kink and antikink can then be written as

$$\begin{aligned} \Phi_{K\bar{K}}(x) &= \frac{[1 - F_K]}{2}\Phi_- + \frac{[1 + F_K]}{2}\Phi_0 \\ &+ \frac{[1 - F_{\bar{K}}]}{2}\Phi_0 + \frac{[1 + F_{\bar{K}}]}{2}\Phi_+ \\ &- \Phi_0, \end{aligned} \quad (40)$$

where $\Phi_- = \Phi_{K\bar{K}}(-\infty)$, $\Phi_0 = \Phi_{K\bar{K}}(0)$, $\Phi_+ = \Phi_{K\bar{K}}(+\infty)$,

$$F_K = \tanh[\sigma\gamma(x+a)], \quad (41)$$

$$F_{\bar{K}} = \tanh[\sigma\gamma(x-a)], \quad (42)$$

and $\gamma = 1/\sqrt{1-v^2}$ is the Lorentz factor.

The total energy of the ansatz (40) is a sum of the gradient and the potential energies obtained by integrating corresponding energy densities along the space direction x :

$$E = G + P, \quad (43)$$

where

$$G = \int_{-\infty}^{+\infty} dx \text{Tr}(\partial_x \Phi_{K\bar{K}})^2, \quad (44)$$

$$\begin{aligned} P &= \int_{-\infty}^{+\infty} dx \left\{ -m^2 \text{Tr}(\Phi_{K\bar{K}})^2 + h (\text{Tr}(\Phi_{K\bar{K}})^2)^2 \right. \\ &\quad \left. + \lambda \text{Tr}(\Phi_{K\bar{K}})^4 + \frac{m^2\eta^2}{4} \right\} \end{aligned} \quad (45)$$

At first let us consider a $q = 2$ kink and a $q = 2$ antikink such that $\Phi_K(-\infty) = \Phi_{\bar{K}}(+\infty)$ (the $q^{(1)} = 2$, $q^{(2)} = 2$, $q^{(3)} = 0$ case in Table I). A possible set of boundary conditions corresponding to this case is:

$$\begin{aligned} \Phi_- &= \frac{\eta}{2\sqrt{15}} \text{diag}(2, 2, 2, -3, -3), \\ \Phi_0 &= \frac{\eta}{2\sqrt{15}} \text{diag}(3, 3, -2, -2, -2), \\ \Phi_+ &= \frac{\eta}{2\sqrt{15}} \text{diag}(2, 2, 2, -3, -3). \end{aligned} \quad (46)$$

Using these boundary conditions in Eq.(40) and substituting latter into Eqns. (44) and (45) gives

$$\begin{aligned} G &= \int_{-\infty}^{+\infty} dX \frac{m^3 \gamma}{\sqrt{2} \lambda} (\partial_X F_K - \partial_X F_{\bar{K}})^2, \\ P &= \int_{-\infty}^{+\infty} dX \frac{m^3}{\sqrt{2} \lambda \gamma} [(F_K - F_{\bar{K}})^4 \\ &\quad - 4(F_K - F_{\bar{K}})^3 + 4(F_K - F_{\bar{K}})^2], \end{aligned} \quad (47)$$

where $X = \gamma m x / \sqrt{2}$ and we have taken $h/\lambda = -3/20$. Evaluating integrals in Eq.(47) and using $R = \sqrt{2} \gamma m a$ yields

$$\begin{aligned} G &= \frac{4\sqrt{2}m^3\gamma}{\lambda} \left[\frac{1}{3} + \frac{\sinh R - R \cosh R}{\sinh^3 R} \right], \\ P &= \frac{4\sqrt{2}m^3}{\lambda\gamma} \left[\frac{1}{3} + \frac{1}{\sinh^3 R} \left\{ e^{-3R} \left(\frac{3}{2} + R \right) \right. \right. \\ &\quad \left. \left. e^{-R} \left(\frac{7}{2} R - \frac{1}{2} \right) + e^R \left(\frac{1}{2} R - 1 \right) \right\} \right]. \end{aligned} \quad (48)$$

As expected, at $R = \infty$ the total energy is equal to the sum of the two kink masses ($2 \times 4\sqrt{2}m^3/(3\lambda)$) [15] divided by the Lorentz factor. Subtracting $E(\infty)$ from $E(R) = G(R) + P(R)$ leaves only the interaction part of the total energy:

$$\begin{aligned} U_0(R) &= \frac{4\sqrt{2}m^3\gamma}{\lambda \sinh^3 R} (\sinh R - R \cosh R \\ &\quad + \frac{1}{\gamma^2} [e^{-3R} (\frac{3}{2} + R) + e^{-R} (\frac{7}{2} R - \frac{1}{2}) \\ &\quad + e^R (\frac{1}{2} R - 1)]) \end{aligned} \quad (49)$$

The dependence of $U_0(R)$ on R for $\gamma = 1$ is shown as a solid line in Fig. 1. It clearly indicates an attraction between the kink and the antikink.

The validity of the ansatz (38) cannot be justified for small values of R . To test the analytical result, we have evaluated the interaction energy numerically by explicitly integrating the full set of equations of motion and evaluating the spatial integral over the gradient and potential energy densities at each time step. The separation R between the kinks was defined as the distance between the maxima of their potential energy densities. The shape of the found interaction potential was similar to the one given by Eq. (49), not only for $h/\lambda = -3/20$, but for all considered values of the parameter: $-7/30 < h/\lambda < 100$. The interaction potential for walls with different values of $\gamma > 1$ was also qualitatively the same.

Next, let us consider the interaction of a $q = 2$ kink and a $q = 2$ antikink but with $\Phi_K(-\infty) \neq \Phi_{\bar{K}}(+\infty)$. This would correspond to the $(q^{(1)} = 2, q^{(2)} = 2, q^{(3)} = 1)$ case in Table I. Keeping Φ_- and Φ_0 the same as in Eq. (46) we can choose Φ_+ to be

$$\Phi_+ = \frac{\eta}{2\sqrt{15}} \text{diag}(2, 2, -3, -3, 2). \quad (50)$$

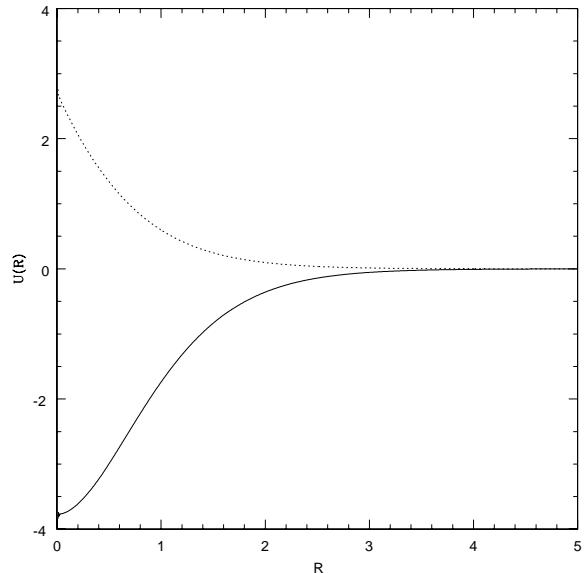


Figure 1: Interaction potentials U_0 , given by Eq. (49) (solid line), and U_1 , given by Eq. (52) (dotted line), for $\gamma = m = \lambda = 1$.

This choice of boundary conditions leads to

$$\begin{aligned} G &= \int_{-\infty}^{+\infty} dX \frac{m^3 \gamma}{\sqrt{2} \lambda} (2\partial_X F_K^2 + \partial_X F_K \partial_X F_{\bar{K}} + 2\partial_X F_{\bar{K}}^2), \\ P &= \int_{-\infty}^{+\infty} dX \frac{m^3}{8\sqrt{2} \lambda \gamma} [8(F_K - F_{\bar{K}})^4 + 8(F_K - F_{\bar{K}})^3 \\ &\quad - 13(F_K - F_{\bar{K}})^2 - 30(F_K - F_{\bar{K}})(1 - F_K F_{\bar{K}}) \\ &\quad + 40F_K F_{\bar{K}}(F_K^2 + F_{\bar{K}}^2 - 2) + 10F_K F_{\bar{K}}(1 - F_K F_{\bar{K}}) \\ &\quad + 35(1 - F_K^2 F_{\bar{K}}^2)]. \end{aligned} \quad (51)$$

Performing the integration and subtracting $E(\infty)$ gives the interaction potential between the two walls:

$$\begin{aligned} U_1(R) &= \frac{\sqrt{2}m^3\gamma}{\lambda \sinh^3 R} (R \cosh R - \sinh R \\ &\quad + \frac{1}{8\gamma^2} [e^{-3R}(3 + 7R) - e^{-R}(11 + 13R) \\ &\quad + e^R(8 - 4R)]) \end{aligned} \quad (52)$$

We find that in this case, the interaction potential is purely repulsive. The dependence of $U_1(R)$ on R for $\gamma = 1$ is shown as a dashed line in Fig. 1. The exact numerical evaluation of the interaction energy of this kink-antikink system, using the method outlined above, did not show qualitative deviations from $U_1(R)$ for all considered values of h/λ and γ .

The two configurations: $(q^{(1)} = 2, q^{(2)} = 2, q^{(3)} = 0)$ and $(q^{(1)} = 2, q^{(2)} = 2, q^{(3)} = 1)$, as well as the well-studied ϕ^4 -equivalent case $(q^{(1)} = 0, q^{(2)} = 0, q^{(3)} = 0)$,

are the only ones for which analytical kink solutions are known. Other configurations from Table I were treated only numerically. For all considered choices of parameters and velocities, we did not see any deviation from the predictions for the attraction or repulsion given in Table I.

V. $SU(5) \times Z_2$ KINK-ANTI-KINK COLLISIONS

In this section we will study kink-antikink collisions. Even in the “simple” case of a ϕ^4 kink colliding with an antikink the variety of possible outcomes is surprisingly rich [5, 6, 7, 8, 9, 10, 12]. Depending on the incident velocity, the two kinks can annihilate, or they can bounce off each other and never meet again, or they can form an intermediate bound state, namely, they can bounce off each other several times before ultimately separating or annihilating. The dependence on the incident velocity is rather non-trivial, as was found in [5, 6, 7, 8, 9, 10] and investigated in detail in [12]. Namely, it was found that, over a relatively small range of initial velocities, intervals of initial velocity for which kink and antikink capture each other alternate with regions for which the interaction concludes with escape to infinite separations. In [12], this alternation phenomenon was attributed to a nonlinear resonance between the orbital frequency of the bound kink-antikink pair and the frequency of characteristic small oscillations of the field localized at the moving kink and antikink centers.

We will not attempt a study of exact dependence of outcomes of kink-antikink collisions on initial velocities. The reason is that in $SU(5) \times Z_2$ there are too many possible combinations and there is an additional parameter, h/λ , which can possibly affect the stability of kink solutions and the outcome of kink-antikink collisions. Instead, we will describe the outcomes for each of the combinations listed in Table I and illustrate the most interesting ones².

In order to study the collisions, we need to integrate the field equations of motion forward in time. Without loss of generality, we can choose the initial kink-antikink configuration to be diagonal [13]. Since equations of motion preserve the diagonal form, one only needs to consider the evolution of four functions: $a(x, t)$, $b(x, t)$, $c(x, t)$ and $d(x, t)$, defined as:

$$\Phi(x, t) = a(x, t)\lambda_3 + b(x, t)\lambda_8 + c(x, t)\tau_3 + d(x, t)Y, \quad (53)$$

where λ_3 , λ_8 , τ_3 and Y are the diagonal generators of $SU(5)$:

$$\lambda_3 = \frac{1}{2}\text{diag}(1, -1, 0, 0, 0),$$

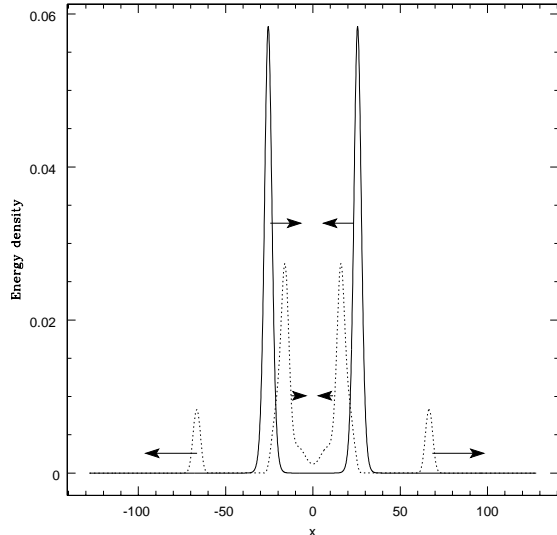


Figure 2: Kink-antikink collision in the ($q^{(1)} = 0$, $q^{(2)} = 0$, $q^{(3)} = 0$) case, in the parameter range when $q = 0$ kink is unstable. The solid line shows the initial energy density profile and the dotted line - the final. The right moving $q = 0$ kink collapsed into a $q = 2$ kink going to the left and the remainder $q = 1$ non-topological ($\epsilon_T = 1$) kink moving to the right. The originally left moving $q = 0$ antikink splits into a right moving $q = 2$ antikink and a left moving $q = 1$ non-topological kink. The arrows show directions and approximate relative magnitudes of kink velocities.

$$\begin{aligned} \lambda_8 &= \frac{1}{2\sqrt{3}}\text{diag}(1, 1, -2, 0, 0), \\ \tau_3 &= \frac{1}{2}\text{diag}(0, 0, 0, 1, -1), \\ Y &= \frac{1}{2\sqrt{15}}\text{diag}(2, 2, 2, -3, -3). \end{aligned} \quad (54)$$

As mentioned in Section III, the $q = 0$ wall is identical to the kink of the simplest ϕ^4 -model. The $q = 0$ solution, however, is known to be locally unstable against perturbations along diagonal components of Φ in the parameter range $h/\lambda > -3/20$ [4]. The outcome of the $q = 0$ kink-antikink collision will, therefore, depend on h/λ as well as on $v_{initial}$. In Fig. 2 and Fig. 3 we illustrate the collision for $v_{initial} = 0.05$ and $h/\lambda = 0$. Just before the collision, both the kink and the antikink collapse. More detailed analysis of functions a , b , c and d in Fig. 3 reveals that the $q = 0$ kink, initially moving to the right, has collapsed into a $q = 2$ kink, moving to the left, and the remainder $q = 1$ non-topological ($\epsilon_T = 1$) kink, moving to the right. The originally left moving $q = 0$ antikink has split into a right moving $q = 2$ antikink and a left moving $q = 1$ non-topological kink. The $q = 2$ kinks will separate to infinities, while the fate of $q = 1$ non-topological kinks needs more explanation. As was found in [13], the $q = 1$ non-topological kink is unstable against a collapse into a pair of $q = 2$ kinks. Therefore, depending on the values of

² Several animated kink collisions can be viewed at <http://theory.ic.ac.uk/~LEP/su5kinks.html>.

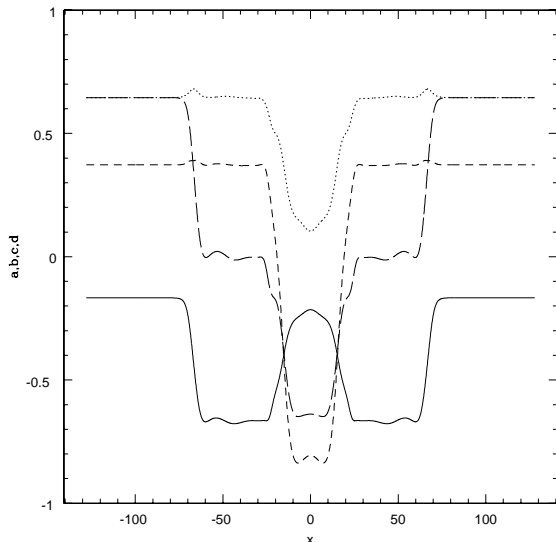


Figure 3: Functions $a(x,t)$ (dotted line), $b(x,t)$ (short dash line), $c(x,t)$ (long dash line) and $d(x,t)$ (solid line), defined in Eq. (53) at the same final snapshot as in Fig. 2.

$v_{initial}$ and h/λ , the non-topological $q = 1$ kinks (in the center of Fig. 2) can either immediately decay into radiation, or they can split into pairs of $q = 2$ kinks moving away from each other. We found that the latter was the case for the choice of parameters corresponding to Fig. 2 and Fig. 3. For $-3/20 < h/\lambda < -3/70$, when $q = 0$ kinks are locally stable, outcomes of their collisions are the same as in the case of kinks and antikinks in ϕ^4 model, the case studied extensively in [5, 6, 7, 8, 9, 10, 11, 12].

Fig. 4 illustrates a collision of a $q = 1$ kink (initially on the left) with a $q = 0$ antikink (initially on the right). The parameters are $v_{initial} = 0.2$, $\eta = 1$, $\lambda = 0.5$ and $h/\lambda = -0.1$. The $q = 0$ kink is unstable for these parameters. The mass of the $q = 0$ kink is $2\sqrt{2}m^3/\lambda'$ [2] and, for our choice of parameters, is equal to 0.243. The $q = 1$ kink mass can only be found numerically and is 0.150. For comparison, the mass of the $q = 2$ kink with these parameters would be 0.033 - almost one fifth the mass of the $q = 1$ kink. We find that, during the collision, the $q = 0$ kink collapses into a $q = 2$ kink traveling to the right and a $q = 1$ non-topological kink traveling to the left. At the same time, the original $q = 1$ kink collapses into three $q = 2$ kinks, with outer kinks moving away from each other. The final configuration is that of four $q = 2$ kinks arranged so that the two left most kinks and the two right most kinks form $(q^{(1)} = 2, q^{(2)} = 2, q^{(3)} = 1)$ combinations, while the two inner kinks form a $(q^{(1)} = 2, q^{(2)} = 2, q^{(3)} = 0)$ combination. The rest of the original energy is radiated away.

In Fig. 5 the initial configuration is $(q^{(1)} = 0, q^{(2)} = 2, q^{(3)} = 2)$. In this case, the $q = 0$ antikink (initially on the right) splits into a $q = 2$ topological antikink, which starts interacting with the $q = 2$ kink, and a $q = 1$

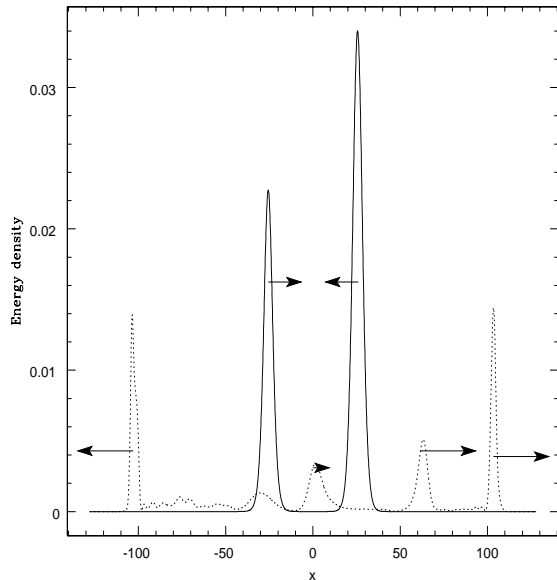


Figure 4: Kink-antikink collision in the $(q^{(1)} = 1, q^{(2)} = 0, q^{(3)} = 1)$ case. The solid line shows the initial energy density profile and the dotted line - the final. After the collision, there are four $q = 2$ kinks arranged so that the left most and the right most pairs of kinks form $(q^{(1)} = 2, q^{(2)} = 2, q^{(3)} = 1)$ combinations and the two inner kinks form a $(q^{(1)} = 2, q^{(2)} = 2, q^{(3)} = 0)$ combination. The rest of the original energy is being radiated away. The arrows show directions and approximate relative magnitudes of kink velocities.

non-topological kink, which keeps propagating to the left unperturbed. Another way to describe this interaction is that the $q = 2$ wall has met its $q = 2$ “reflection” in the $q = 0$ wall and formed a complex with it, while the remainder wall is radiated away.

The $(q^{(1)} = 1, q^{(2)} = 1, q^{(3)} = 0)$ case has essentially the same set of possible outcomes as the $(q^{(1)} = 0, q^{(2)} = 0, q^{(3)} = 0)$ and will not be considered here.

Fig. 6 illustrates the outcome of the kink-antikink collision with the initial $(q^{(1)} = 1, q^{(2)} = 1, q^{(3)} = 1)$ configuration. The parameters were chosen to be $h/\lambda = -0.1$ and $v_{initial} = 0.2$. The final configuration is that of two $q = 2$ kinks, arranged in a $(q^{(1)} = 2, q^{(2)} = 2, q^{(3)} = 1)$ combination, moving away from each other.

The outcome of a $(q^{(1)} = 1, q^{(2)} = 1, q^{(3)} = 2)$ collision with $h/\lambda = -0.1$ and $v_{initial} = 0.2$ is shown in Fig. 7. The final configuration is that two $(q^{(1)} = 2, q^{(2)} = 2, q^{(3)} = 1)$ combinations moving away from each other.

The $(q^{(1)} = 1, q^{(2)} = 2, q^{(3)} = 1)$ case with $h/\lambda = -0.1$ and $v_{initial} = 0.1$ is illustrated in Fig. 8. Just before the collision, the $q = 1$ kink (originally on the left) collapses into three $q = 2$ kinks, with two outer kinks having large kinetic energies. Thus, an intermediate configuration is that of four $q = 2$ kinks, including the initial one (originally on the right). The two right most $q = 2$ kinks are in a $(q^{(1)} = 2, q^{(2)} = 2, q^{(3)} = 0)$ combination and, depend-

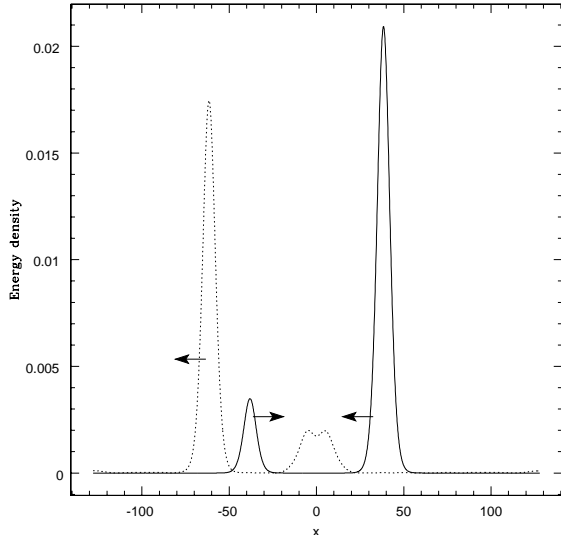


Figure 5: Kink-antikink collision in the $(q^{(1)} = 0, q^{(2)} = 2, q^{(3)} = 2)$ case. Resulting configuration (dotted line) is that of a non-topological $q = 1$ kink moving to the left, while the $q = 2$ kink has captured its “mirror image” (the $q = 2$ antikink) originally contained in the incident $q = 1$ wall.

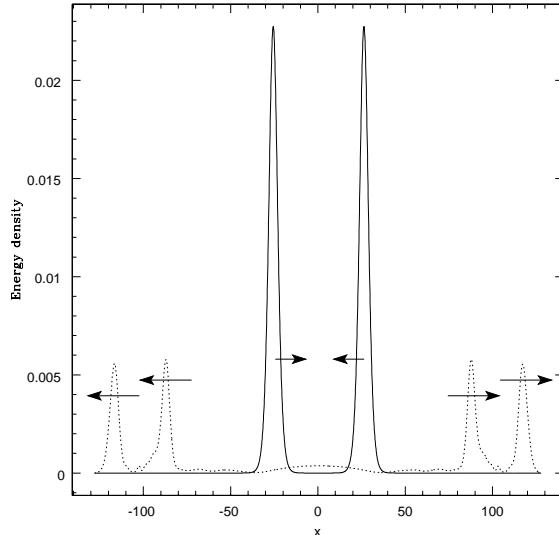


Figure 7: The $(q^{(1)} = 1, q^{(2)} = 1, q^{(3)} = 2)$ case with $h/\lambda = -0.1$ and $v_{initial} = 0.2$. The final configuration is that two $(q^{(1)} = 2, q^{(2)} = 2, q^{(3)} = 1)$ combinations moving away from each other.

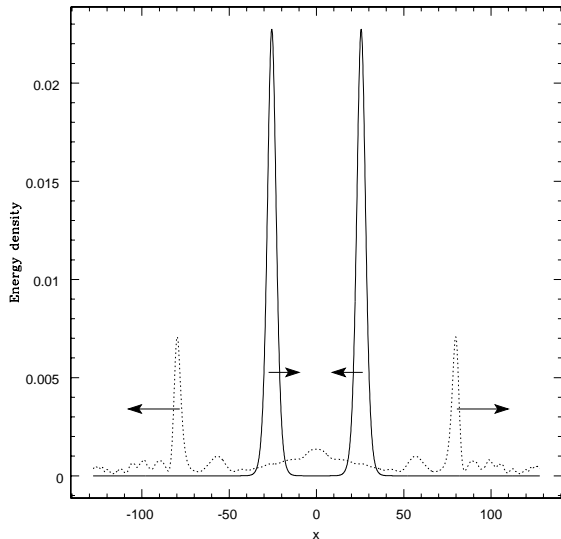


Figure 6: The $(q^{(1)} = 1, q^{(2)} = 1, q^{(3)} = 1)$ case with $h/\lambda = -0.1$ and $v_{initial} = 0.2$. The final configuration is that of two $q = 2$ kinks, arranged in a $(q^{(1)} = 2, q^{(2)} = 2, q^{(3)} = 1)$ combination, moving away from each other.

ing on the initial velocity, may annihilate or chase each other forever. The two left most walls are in a $(q^{(1)} = 2, q^{(2)} = 2, q^{(3)} = 1)$ arrangement.

A $q^{(1)} = 1$ kink and a $q^{(2)} = 2$ antikink arranged in a $(q^{(1)} = 1, q^{(2)} = 2, q^{(3)} = 2)$ combination repel. For $h/\lambda = -0.1$ and $v_{initial} = 0.15$ they scatter elastically.

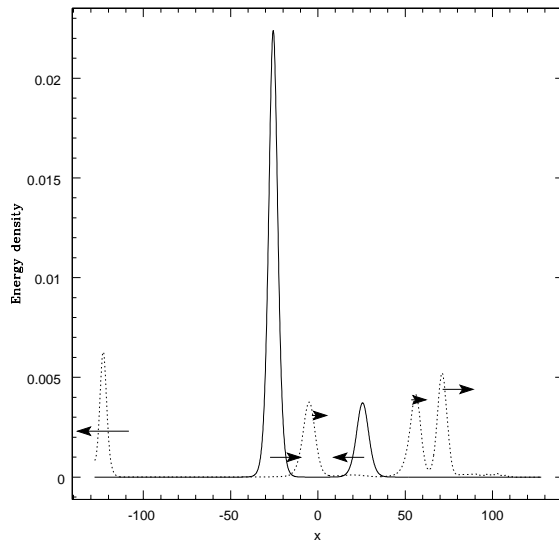


Figure 8: The $(q^{(1)} = 1, q^{(2)} = 2, q^{(3)} = 1)$ case with $h/\lambda = -0.1$ and $v_{initial} = 0.1$. There are four $q = 2$ kinks left as a result of the collision.

The lighter $q = 2$ kink (initially on the right) bounces off the heavier $q = 1$ kink and slows it down.

The remaining two combinations from Table I are $(q^{(1)} = 2, q^{(2)} = 2, q^{(3)} = 0)$ and $(q^{(1)} = 2, q^{(2)} = 2, q^{(3)} = 1)$. Since these are the only two initial combinations that involve stable kinks and antikinks, they would be the most important ones if one studied evolution of domain wall networks after the formation. How-

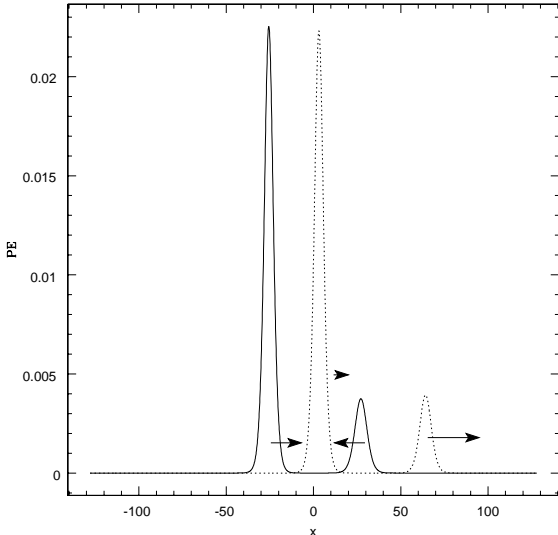


Figure 9: The elastic scattering in the $(q^{(1)} = 1, q^{(2)} = 2, q^{(3)} = 2)$ case with $h/\lambda = -0.1$ and $v_{initial} = 0.1$.

ever, these two are also the most “uninteresting” combinations from the novelty point of view. In the case of $(q^{(1)} = 2, q^{(2)} = 2, q^{(3)} = 0)$, the dynamics and possible outcomes are qualitatively identical to the case of kink-antikink collision in the simple ϕ^4 model. Namely, we observe a dependence on the incident velocity similar to that found in Refs. [5, 6, 7, 8, 9, 10, 12]. The difference is that in the case of $SU(5)$ the value of the incident velocity leading to a given outcome depends on the parameter h/λ of the potential given in Eq. (33).

In the $(q^{(1)} = 2, q^{(2)} = 2, q^{(3)} = 1)$ case, the kink and antikink repel and simply bounce off each other elastically.

VI. SUMMARY AND DISCUSSION

As we have illustrated in the previous sections, kink-antikink interactions in $SU(N) \times Z_2$ can be of different types with many possible outcomes depending on the choice of the parameter values.

In order to see how a pair of kinks will interact, one generally needs to specify the potential $V(\Phi)$ and evaluate the interaction energy between the two kinks. However, we have shown that to a very good approximation the nature of the interaction can be determined by evaluating $\text{Tr}[Q^{(1)}Q^{(2)}]$, where $Q^{(1)}$ and $Q^{(2)}$ are the charges of the two kinks defined by Eq. (10). In particular, we have shown that kinks and antikinks may attract or repel depending on their relative orientation in the internal space. This is similar to interactions between global $O(3)$ monopoles, where the relative phase, not the topological charges, is what determines the nature of the interaction

[17].

In our study of kink-antikink collisions in $SU(5) \times Z_2$ we have seen a general tendency for larger mass topological kinks to split into fundamental kinks of the theory, such as the $q = 2$ kink. This suggests that kink-antikink interactions in $SU(N) \times Z_2$ can be described in terms of interactions between fundamental (*i.e.* globally stable) $q = (N - 1)/2$ kinks. Namely, given the configuration of two kinks, one would look for the least energy configuration of $q = n$ kinks that would have the same global topology as the original pair of kinks. The outcome of the interaction would then be reduced to interactions between attractive or repulsive pairs of $q = n$ kinks.

We have not investigated the detailed dependence of the dynamics of kink-antikink collisions on the initial velocities. Part of the reason is that the outcome strongly depends on the stability properties of each of the solitons and our numerical methods do not give us the possibility of properly accounting for all instabilities that can occur in the model. Each kink, except for the fundamental one, is unstable in a different way, namely, along a different direction in the internal space of $SU(5)$, and also depends on the particular choice of the potential. It is possible that a more detailed study would reveal a connection with earlier work on Q balls [18] and global $U(1)$ strings [19], where it was observed that at very high collision velocities fragmentation of solitons is generally suppressed. Such a study could be a subject of future work.

From the equations of motion it follows that if the Higgs field components along non-diagonal generators of $SU(5)$ were zero at the initial time, they would remain zero at all times, which was the case in our simulations. However, except for the $q = 2$ topological kinks, kink solutions can be unstable against perturbations along non-diagonal generators of $SU(5)$ [13]. In a realistic domain wall formation scenario one would have to allow for all components of the Higgs to be excited and only stable walls would survive. Depending on the rate of the phase transition, temporary formation of unstable kinks will or will not be relevant. Nevertheless, stable and unstable kinks are solutions of the classical field equations and their interactions may become important whenever an exact or approximate $SU(N) \times Z_2$ symmetry is present in a theory.

Acknowledgments

I would like to thank Tanmay Vachaspati for several important insights and for commenting on the earlier draft of the manuscript. I am grateful to N. Antunes, J. Kalkkinen and T. W. B. Kibble for useful discussions. Conversations with participants of the ESF COSLAB Programme workshop at Imperial College in July, 2001, and especially with F. A. Bais and L. Perivolaropoulos, are acknowledged. This work was supported by PPARC.

-
- [1] A. Vilenkin and E. P. S. Shellard, *“Cosmic strings and other topological defects”*, Cambridge University Press, first paperback edition (2000).
- [2] R. Rajaraman, *“Solitons and Instantons”*, North-Holland (1987).
- [3] T. Vachaspati, Phys. Rev. Lett. **76**, 188 (1996).
- [4] G. Dvali, H. Liu, T. Vachaspati, Phys. Rev. Lett. **80** 2281 (1998).
- [5] A. E. Kudryavtsev, JETP Lett. **22**, 82 (1975);
- [6] A. Aubry, J. Chem. Phys. **64**, 3392 (1976);
- [7] V. G. Makhankov, Phys. Repts. **35C** 1, (1978);
- [8] C. A. Wingate, Ph.D. Thesis, University of Illinois (1978); and SIAM J. Appl. Math. **43**, 120 (1983);
- [9] M. J. Ablowitz, M. D. Kruskal and J. R. Ladik, SIAM J. Appl. Math. **36**, 478 (1979);
- [10] M. Moshir, Nucl. Phys. **B185**, 318-332 (1981).
- [11] T. Sugiyama, Prg. of Theor. Phys. **61**, No.5, 1551 (1979).
- [12] D. Campbell, J. Schonfeld, and C. Wingate, Physica **9D**, 1-32 (1983).
- [13] L. Pogosian and T. Vachaspati, Phys. Rev. **D64**, 105023 (2001).
- [14] N. S. Manton, Nucl. Phys. **B150**, 397 (1979)
- [15] T. Vachaspati, Phys. Rev. **D63**, 105010 (2001).
- [16] L. Pogosian and T. Vachaspati, Phys. Rev. **D62**, 123506 (2000).
- [17] L. Perivolaropoulos, Nucl. Phys. **B375**, 665 (1992)
- [18] M. Axenides, S. Komineas, L. Perivolaropoulos, M. Floratos, Phys. Rev. **D61**, 085006 (2000).
- [19] E. P. S. Shellard, Nucl. Phys. **B283**, 624 (1987).